

# Two-heavy impurities immersed in squeezed light-boson systems

R. M. Francisco,<sup>1</sup> D. S. Rosa,<sup>2</sup> and T. Frederico<sup>2</sup>

<sup>1</sup>*Universidade Federal de São João del Rei, DCNAT, 36301-160 São João del Rei, MG, Brazil*

<sup>2</sup>*Instituto Tecnológico de Aeronáutica, DCTA, 12228-900 São José dos Campos, SP, Brazil*

We investigate the spectrum and structure of two-heavy bosonic impurities immersed in a light-boson system in  $D$  dimensions by means of the Born-Oppenheimer approximation. The fractional dimension dependence are associated with squeezed traps. The binding energies follows an Efimov type geometrical scaling law when the heavy-light system has a s-wave resonant interaction and the effective dimension or trap deformation is within a given range. The discrete scaling parameter  $s$  relates two consecutive many-body bound states depending on mass asymmetry, number of light-bosons and effective dimension  $D$ . Furthermore, the spectrum and wave-function for finite heavy-light binding energies are computed. To exemplify our results, we consider mixtures of two-heavy caesium atoms interacting with up to two-lithium ones, which are systems of current experimental interest.

## I. INTRODUCTION

The Efimov effect appears in three-body systems that interact by means of short-range resonant forces, leading to an infinite tower of weakly bound states which follows universal geometrical scaling laws close to the three-body threshold [1]. This effect was originally proposed in the nuclear physics context, however, its first evidence was found by Kraemer et al. [2] in trapped ultracold atomic systems. In their work, the Feshbach resonance technique was applied to an ultracold gas of caesium atoms, where they observed a giant three-body recombination loss when the strength of the two-body interaction was varied and the weakly bound Efimov state turned into a continuum resonance (see also [3, 8]). Nowadays, it is known that the Efimov effect is present in several systems, such as atomic gases [9], polarons [10], dipolar molecules [11], strong interacting photons [12] and in general atomic and nuclear physics contexts [13–17].

The Efimov effect is closely related to the collapse of the three-body bound energy discovered by Thomas in 1935 [18]. By decreasing the range of the interaction, Thomas found that the three-body bound state problem admits a solution at any energy with a spectrum “unbounded from below”. Both phenomena are affected by changes in the effective dimension  $D$  in which the system is embedded, for example, just as the Thomas collapse, the Efimov effect is also absent in  $D = 2$ . It has been theoretically demonstrated for homonuclear systems that the Efimov effect survives only for dimensions in the range  $2.3 < D < 3.8$  [13]. Considering heteronuclear systems at the unitary limit, where the two-body binding energies vanish, recent works have shown how the mass imbalance changes the range of dimensions where the Efimov effect is present [19–21]. This was also studied for finite two-body energies [22, 23].

Although technically simple to implement, the  $D$ -dimensional approach in few-body calculations presents a key issue in practice, i.e., the connection to the trap deformation. Recently, it was suggested in [24] an approximate relation between the non-integer dimension  $D$ , and

the trap geometry deformed in one direction by a harmonic potential

$$b_{ho}^2/r_{2D}^2 = 3(D-2)/(3-D)(D-1), \quad (1.1)$$

where  $b_{ho}$  is the oscillator length and  $r_{2D}$  is the root mean square radius of the three-body system in two-dimensions. Despite the advances that led to the possibility to compress and expand the atomic cloud creating effectively two- [25] and one-dimensional [26] setups, to the best of our knowledge, there is not yet experiments designed to measure the effect of continuous changing the trap geometry in the Efimov discrete scaling.

Besides the Efimov effect, in the literature there are studies on the universal properties for more than three-particles in three-dimensions close to the unitarity [27–34]. For a four-boson system, a universal correlation between the binding energies of successive tetramers for large two-body scattering lengths was discovered. By solving the Faddeev-Yakubovsky (FY) equations with zero-range interaction, the findings corroborates with the existence of a four-body limit-cycle beyond the Efimov one [34]. Following that, the shift in the four-body recombination peaks due to the effective-range correction close to the unitary limit was studied [35], explaining experimental observations for the ultracold gas of caesium atoms close to broad Feshbach resonances.

Recently, by means of the Born-Oppenheimer approximation with extreme mass imbalance [36], the independence between few-body scales beyond the Van der Waals universality was demonstrated for many-boson systems composed by two heavy-atoms interacting with  $(N-2)$ -light ones at the unitary. The many-body bound states exhibited independent limit-cycles, each one associated with a given number of light-bosons. A study of the many possibilities of mass imbalanced tetramers was proposed in Ref. [37].

In the present work, we extend the investigation of the many-boson system in [36] by embedding it in an environment defined by an effective dimension  $D$ , which subsequently is associated with trap deformation. It is also varied the mass imbalance and the number of light-atoms to study how these changes impact the geometrical

ratio of consecutive bound states of the system. In addition to results presented for the unitary-limit, we also analyse finite-range corrections for the many-body spectrum. To accomplish this, we obtain an expression for the two-body bound energy as a function of the scattering length and effective dimension  $D$ , which can provide a more directly way to link theoretical to experimental results. Besides that, we obtain the wave function of the two-heavy atoms, as well as an analytical expression for the wave function of the  $(N - 2)$ -lighter atoms, where  $N$  is the total number of particles in the system.

The work is organized as follows. In section II, we present the Born-Oppenheimer formalism used to solve the bound state problem of two-heavy impurities within the system of light-bosons embedded in an effective dimension  $D$  that mimics squeezed traps. Besides that, we analytically compute the  $(N - 2)$ -light bosons wave function, which can be used to parametrize the many-body large-distance tail of the total wave function, and explicitly write the scaling parameter related with successive ratios of many-body bound states for different mass ratios and dimensions considering zero bound heavy-light energies. For three-body systems, the results are compared with the ones found by solving the Skorniakov and Ter-Martirosyan equations. In section III, for the two-heavy impurities, we present bound state energies and wave functions considering corrections of finite heavy-light bound energies. We focus in the limit of discrete scale symmetry to the point where the continuum one takes place. Correlations between the many-body bound state energies as functions of dimension and mass imbalance are discussed as possible limit-cycles. Finally, we apply the present approach to molecules of  ${}^6\text{Li}_{N-2} - {}^{133}\text{Cs}_2$  for  $N = 3$  and  $N = 4$ . In section IV, we summarize our work.

## II. BORN-OPPENHEIMER APPROACH

In this section, we present the formalism used to study the many-body system composed by two heavy-particles with masses  $m_A$  and  $(N - 2)$ -light bosonic atoms with masses  $m_B$  embedded in  $D$ -dimensions. This system is depicted in figure 1.

We are interested in the relative motion between the particles of the system, so that, ignoring the movement of the center of mass, the Hamiltonian can be written in relative coordinates as

$$H = -\frac{\hbar^2}{2\mu_{AA}}\nabla_R^2 + V_B(|\mathbf{R}|) + \sum_{i=1}^{N-2} \left( -\frac{\hbar^2}{2\mu_{B,AA}}\nabla_{r_i}^2 + \sum_{j=1}^2 V_A \left( \left| \mathbf{r}_i + (-1)^j \frac{\mu_{AA}}{m_A} \mathbf{R} \right| \right) \right), \quad (2.1)$$

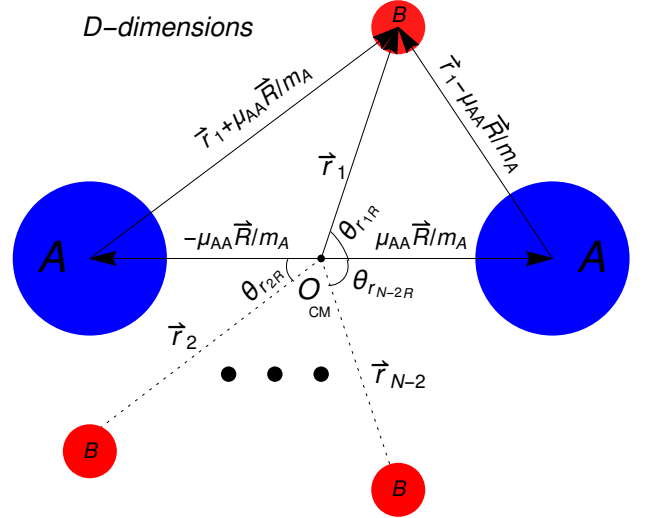


FIG. 1. Representation of the AABBB...B structure forming the  $N$ -body system composed by two identical heavy-atoms with masses  $m_A$ , and  $(N - 2)$  light-atoms with masses  $m_B$ .

where  $\mu_{AA} = m_A/2$  and  $\mu_{B,AA} = 2m_A m_B / (2m_A + m_B)$  are the reduced masses of the system, while  $V_A$  and  $V_B$  denote the  $AB$  and  $AA$  two-body interactions, respectively.

In order to apply the BO approximation, let us consider  $m_B \ll m_A$ . Within this approach, the total wave function of the system  $\Psi(\mathbf{r}_1, \mathbf{r}_2, \dots, \mathbf{r}_{N-2}, \mathbf{R})$  can be written as a product of the wave functions of the  $N - 2$  modes of fast-atoms ( $\psi$ ) and of the slow ones ( $\phi$ ) as

$$\Psi(\mathbf{r}_1, \mathbf{r}_2, \dots, \mathbf{r}_{N-2}, \mathbf{R}) = \phi(\mathbf{R}) \prod_{i=1}^{N-2} \psi_R(\mathbf{r}_i). \quad (2.2)$$

It is worth mentioning here that the total wave function is symmetric under the interchange of the heavy atoms. As the interaction is not dependent on the spin, the formalism developed here may be suitable to describe a many-body system formed by heavy impurities of bosonic or fermionic character in antisymmetric spin states.

In the lowest order approximation, the action of the Laplace operator  $\nabla_R^2$  on the total wave function  $\Psi$  in the Schrodinger equation can be written as

$$\nabla_R^2 \left[ \phi(\mathbf{R}) \prod_{i=1}^{N-2} \psi_R(\mathbf{r}_i) \right] \approx \prod_{i=1}^{N-2} \psi_R(\mathbf{r}_i) \nabla_R^2 \phi(\mathbf{R}). \quad (2.3)$$

Here, it is possible to make this approximation because the other terms generated by the operator action are suppressed by the mass factor ratio. By adopting the BO approximation and our particular choice of Hamiltonian where the light-light potential vanishes, we can write two independent equations for each light particle and for the

heavy ones as

$$\left[ -\frac{\hbar^2 \nabla_{\mathbf{r}_i}^2}{2\mu_{B,AA}} + \sum_{j=1}^2 V_A \left( \left| \mathbf{r}_i + (-1)^j \frac{\mathbf{R}}{2} \right| \right) \right] \psi_R(\mathbf{r}_i) = \epsilon(R) \psi_R(\mathbf{r}_i), \quad (2.4)$$

and

$$\left[ -\frac{\hbar^2 \nabla_{\mathbf{R}}^2}{2\mu_{AA}} + V_B(|\mathbf{R}|) + (N-2)\epsilon(R) \right] \phi(\mathbf{R}) = E_N \phi(\mathbf{R}), \quad (2.5)$$

respectively. The eigenvalue  $\epsilon(R)$  of the Eq. (2.4), depends on the relative position of the heavy-atoms and enters as an effective potential in Eq. (2.5), while the eigenvalue of the heavy-atoms equation gives the many-body energy  $E_N$ .

### A. Light-particle dynamics

In the present model, the zero-range potential acts only in the heavy-light system, and from that an analytical expression for  $\epsilon(R)$  can be obtained. This expression was first derived in the context of three-body systems in  $D$ -dimensions [22], and, as there is no interactions between the light fast-atoms, it can be used in the present study. The energy eigenvalue of the light bosons comes from the solution of a transcendental equation, given by

$$2^{\frac{D}{2}} \left( \frac{\sqrt{|\bar{\epsilon}(\bar{R})|}}{\bar{R}} \right)^{\frac{D-2}{2}} K_{\frac{D-2}{2}} \left( \bar{R} \sqrt{|\bar{\epsilon}(\bar{R})|} \right) - \frac{\pi \csc(D\pi/2)}{\Gamma(D/2)} \left( 1 - |\bar{\epsilon}(\bar{R})|^{\frac{D-2}{2}} \right) = 0, \quad (2.6)$$

where  $|\bar{\epsilon}(\bar{R})| = |\epsilon(R)|/|E_2^{(D)}|$  and  $|E_2^{(D)}|$  is the two-body bound state energy of each pair of heavy-light atoms. The dimensionless relative distance between the heavy atoms is  $\bar{R} = R/L$ , with  $L = \sqrt{\hbar^2/2\mu_{B,AA}|E_2^{(D)}|}$ .  $K_\alpha(z)$  and  $\Gamma(z)$  are the modified Bessel function of the second kind and the gamma function, respectively.

The effective potential between the heavy-particles from the solution of Eq. (2.6) assumes quite simple forms in the limits of large and small distances  $\bar{R} \gg 1$  and  $\bar{R} \ll 1$ . These forms are given by

$$\lim_{\bar{R} \rightarrow \infty} |\epsilon(R)| = |E_2^{(D)}| + |E_2^{(D)}| K_{\frac{D-2}{2}}(\bar{R}) \frac{2^{\frac{(D+2)}{2}} \Gamma(D/2) \bar{R}^{\frac{2-D}{2}}}{(2-D)\pi \csc(D\pi/2)}, \quad (2.7)$$

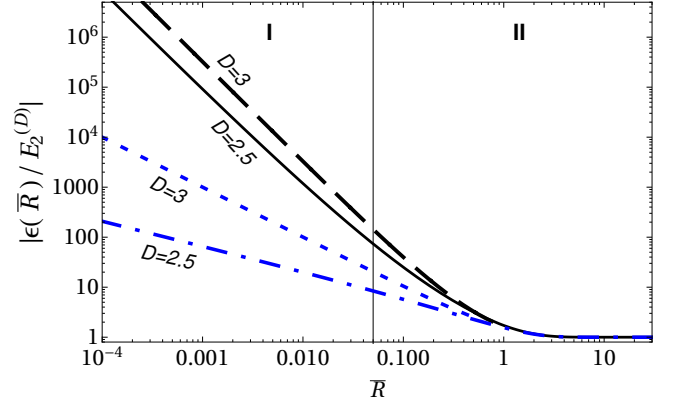


FIG. 2. Effective potential between the two heavy atoms as a function of the dimensionless distance,  $\bar{R} = R/L$  ( $L = [\hbar^2/2\mu_{B,AA}|E_2^{(D)}|]^{\frac{1}{2}}$ ). The results for the effective potential from the solution of Eq. (2.6) are presented for  $D = 3$  (black long-dashed line) and  $D = 2.5$  (black solid line). The asymptotic form of the potential at large distances ( $\bar{R} \gg 1$ ) from Eq. (2.7) are shown for  $D = 3$  (blue short-dashed line) and  $D = 2.5$  (blue dot-dashed line). Regions I and II are separated by the vertical line and region I corresponds to  $\bar{R} \ll 1$  where the potential is dominated by the asymptotic form given in Eq. (2.8) with  $g(D = 3) = -0.322$  and with  $g(D = 2.5) = -0.081$ .

and

$$\lim_{\bar{R} \rightarrow 0} |\epsilon(R)| = \frac{\hbar^2 g(D)}{2\mu_{B,AA} \bar{R}^2}, \quad (2.8)$$

where  $g(D)$  is the solution of the transcendental equation

$$g(D) = \left[ -\frac{\pi \csc(D\pi/2)}{2^{\frac{D}{2}} \Gamma(D/2) K_{\frac{D-2}{2}}(\sqrt{g(D)})} \right]^{\frac{4}{2-D}}. \quad (2.9)$$

At the unitary limit, for any finite distance between the heavy atoms, only the contribution proportional to  $1/\bar{R}^2$  from Eq. (2.8) survives. This form of the potential allows the presence of the Thomas collapse for dimensions  $2 < D < 4$ , restricted to conditions of mass configuration and effective dimension  $D$ . For illustration, in Fig.2 we plot the effective potential between the two heavy atoms for two different dimensions. Basically, the value of the two-body energy defines the tail of the potential, and the relative distance in which the two-heavy atoms are under the action of the inverse square interaction. In the unitary limit, region II disappears, and we have the  $g(D)/\bar{R}^2$  behaviour of the effective potential represented in region I, as clearly seen in the figure.

We will now turn our attention to the wave function of the light fast-atoms. The Fourier transform of  $\psi_R(\mathbf{p}_i)$  can be analytically calculated from

$$\psi_R(\mathbf{r}_i) = \int \frac{d^D p_i}{(2\pi)^D} \frac{e^{i\mathbf{p}_i \cdot (\mathbf{r}_i + \mathbf{R}/2)} + e^{i\mathbf{p}_i \cdot (\mathbf{r}_i - \mathbf{R}/2)}}{\epsilon(R) - p_i^2/\mu_{B,AA}}, \quad (2.10)$$

which gives

$$\begin{aligned} \psi_R(\mathbf{r}_i) = & -\frac{2\mu_{B,AA}}{\hbar^2(2\pi)^{\frac{D}{2}}} \left( \sqrt{\frac{2\mu_{B,AA}|\epsilon(R)|}{\hbar^2}} \right)^{\frac{D-2}{2}} \\ & \times \left[ \left( \left| \mathbf{r}_i + \frac{\mathbf{R}}{2} \right| \right)^{\frac{2-D}{2}} K_{\frac{D-2}{2}} \left( \sqrt{\frac{2\mu_{B,AA}|\epsilon(R)|}{\hbar^2}} \left| \mathbf{r}_i + \frac{\mathbf{R}}{2} \right| \right) \right. \\ & \left. + \left( \left| \mathbf{r}_i - \frac{\mathbf{R}}{2} \right| \right)^{\frac{2-D}{2}} K_{\frac{D-2}{2}} \left( \sqrt{\frac{2\mu_{B,AA}|\epsilon(R)|}{\hbar^2}} \left| \mathbf{r}_i - \frac{\mathbf{R}}{2} \right| \right) \right]. \end{aligned} \quad (2.11)$$

Close to the unitary limit, the wave function simplifies to

$$\begin{aligned} \psi_R(r_i) = & -\frac{R^{2-D}}{(2\pi)^{\frac{D}{2}}} \frac{2\mu_{B,AA}}{\hbar^2} g(D)^{\frac{D-2}{4}} \\ & \times \left[ \zeta_+^{\frac{2-D}{4}} K_{\frac{D-2}{2}} \left( \sqrt{g(D)} \zeta_+ \right) + \zeta_-^{\frac{2-D}{4}} K_{\frac{D-2}{2}} \left( \sqrt{g(D)} \zeta_- \right) \right], \end{aligned} \quad (2.12)$$

where

$$\zeta_{\pm} = \frac{r_i^2}{R^2} + \frac{1}{4} \pm \frac{r_i}{R} \cos(\theta_{r_i R}). \quad (2.13)$$

We observe that, besides  $R$ , there is no other scale present in the light-atom wave function, which is expected in the unitary limit.

In figure 3, we show the results for the light-particle wave function for the mass ratio of  ${}^6\text{Li}$  and  ${}^{133}\text{Cs}$  embedded in two different dimensions, namely  $D = 3$  and  $2.5$ , in the last case, trap geometry  $b_{ho}/r_{2D} = 1.414$ . In the upper panel, we have an overall view of the light-particle wave function. The peak at  $r_i/R = 1/2$  and  $\cos(\theta_{r_i R}) = \pm 1$  comes from the logarithmic divergence of the Bessel function  $K_{\frac{D-2}{2}}$  when its argument approaches zero, and, as the wave function is symmetric around  $\cos(\theta_{r_i R}) = 0$ , it is localized for angles close to  $0^\circ$  and  $180^\circ$ . Such situation corresponds to the light-particle being at the top of one of the heavy-particles. It is noticeable that the large distance behavior of the light-particle wave function for  $D = 3$  decreases faster than for  $D = 2.5$ . In the lower panel of the figure, we detail the behavior of the wave function with  $r_i/R$  for two fixed values of  $\cos(\theta_{r_i R})$  (1 and 0.8) and  $D$  (2.5 and 3). The results are arbitrarily normalized to be 1 for  $r_i/R = 1$  and  $\cos(\theta_{r_i R}) = 1$ . Two properties seen in the upper panel are evident in this figure: (i) the peak vanishes fast by decreasing the cosine and (ii) the exponential tail of the wave function is less damped for  $D = 2.5$  than for  $D = 3$ .

### B. Heavy-particles dynamics

We now study the many-body bound-state properties by solving the energy eigenvalue equation for the heavy

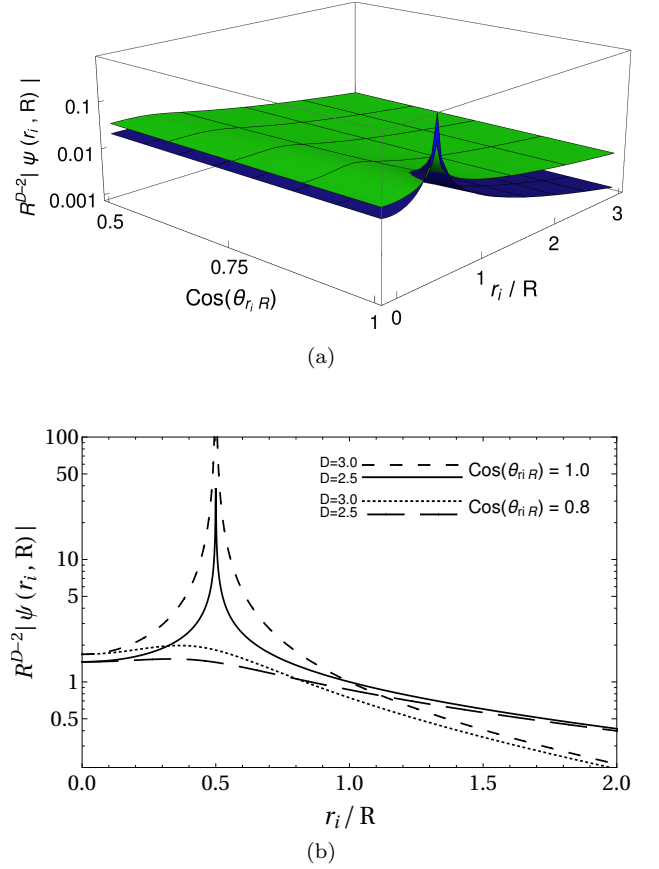


FIG. 3. Upper panel: wave function of each light-atom in the system  ${}^6\text{Li}_{N-2}-{}^{133}\text{Cs}_2$  considering two different dimensions  $D = 3$  (blue surfaces) and  $D = 2.5$  (green surface) or, in the last case, trap geometry  $b_{ho}/r_{2D} = 1.414$ . Lower panel: wave function for fixed  $\cos\theta_{r_i R}$  and different dimensions as a function of the ratio  $r_i/R$ .

pair. The solutions are determined by the two-body energy  $E_2^{(D)}$ , the mass ratio  $m_B/m_A$ , the angular momentum  $l$ , the effective dimension  $D$  and the number of light-atoms presented in the system. Furthermore, in the situation where the Thomas collapse is present, it is necessary to introduce a short-range regularization of the effective potential.

By defining a reduced wave function,  $\chi(R)$ , through  $\phi(R) = \chi(R)/R^{(D-1)/2}$  and considering the presence of  $(N-2)$ -light atoms to generate the effective potential between the heavy ones, the corresponding energy eigenvalue equation in the relative coordinate, Eq. (2.5), can be rewritten as

$$\begin{aligned} \left[ -\frac{d^2}{dR^2} - (N-2) \frac{m_A}{\hbar^2} \epsilon(R) + \frac{(D-3+2l)(D-1+2l)}{4R^2} \right. \\ \left. + \frac{m_A}{\hbar^2} V_B(R) \right] \chi(R) = \frac{m_A}{\hbar^2} E_N^{(D)} \chi(R), \end{aligned} \quad (2.14)$$

where  $l$  is the total angular momentum. For identical heavy atoms in the same spin state,  $l$  will be even for bosons and odd for fermions.

### 1. Unitary limit

First, we turn off the heavy-heavy interaction ( $V_B = 0$ ) to investigate the many-body problem at the unitary limit, where the effective potential given in Eq. (2.8) is attractive and proportional to  $1/R^2$  with a strength that depends on the mass ratio  $m_B/m_A$  and dimension  $D$ . Under the situation of the Landau fall to the center [38], we can consider the most excited state where  $E_N^{(D)}$  is close to zero, so that the heavy particles eigenvalue equation (2.14) becomes

$$\left[ -\frac{d^2}{dR^2} - \frac{m_A}{2\mu_{B,AA}}(N-2)\frac{g(D)}{R^2} + \frac{(D-3+2l)(D-1+2l)}{4R^2} \right] \chi(R) = 0. \quad (2.15)$$

Assuming an ansatz for the heavy-atoms reduced wave function as  $\chi(R) = R^\delta$ , we can write a second order equation

$$-\delta(\delta-1) - \frac{m_A}{2\mu_{B,AA}}(N-2)g(D) + \frac{(D-3+2l)(D-1+2l)}{4} = 0, \quad (2.16)$$

whose solutions have the form  $\delta = 1/2 \mp is$ , with

$$s = \sqrt{\frac{m_A}{2\mu_{B,AA}}(N-2)g(D) - \frac{(D-2+2l)^2}{4}}, \quad (2.17)$$

where  $s$  can be either real or imaginary, depending on the mass ratio, angular momentum, dimension and number of light-atoms.

The condition for the manifestation of log-periodic oscillations in  $\chi(R)$  is that  $s$  must be real. In this case the continuous scale invariance is broken to a discrete one. In the situation that Eq. (2.17) results in  $s$  purely imaginary, the continuous scale invariance is restored and the nature of the system belongs to "unparticle" physics [39], which will be not further explored in this work.

To obtain real values of  $s$  we have to satisfy the inequation

$$\frac{m_A}{2\mu_{B,AA}}(N-2)g(D) > \frac{(D-2+2l)^2}{4}. \quad (2.18)$$

The expression above defines surfaces for the critical dimension where the geometrical scaling regime vanishes as a function of  $l$  and  $N$  for a given mass ratio. In Fig. 4, it is shown two of these surfaces, standing for light-heavy mass ratios of 0.1 (cyan) and 6/133 (blue). Once the mass ratio decreases, the region for the manifestation of geometrical scaling law is known to enlarge, a property that is kept by changing dimensions. By increasing the

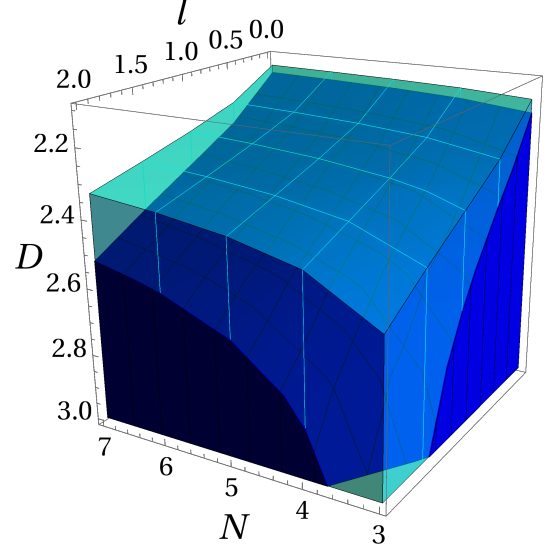


FIG. 4. Regions for the existence of the Efimov effect in the unitary limit for different dimensions, angular momentum and number of light-atoms. Lower blue and upper cyan regions presents results for  $m_B/m_A = 6/133$  and  $m_B/m_A = 0.1$ , respectively.

number of light-bosons, the maximum value of angular momentum that allows the existence of the discrete geometrical scaling parameter increases, while lower values of  $D$  or larger trap asymmetries becomes accessible for this regime.

We can go forward in the exploration of the many-body system. Replacing the value of  $s$  in Eq. (2.15) for finite bound state energies, allow us to write a differential equation of the form

$$\left[ -\frac{d^2}{dR^2} - \frac{s^2 - 1/4}{R^2} \right] \chi(R) = -\kappa^2 \chi(R), \quad (2.19)$$

where  $m_A E_N^{(D)}/\hbar^2 = -\kappa^2$ . Looking for the bound state solution and implementing the corresponding boundary condition, one finds that

$$\chi(R) = \sqrt{R} K_{is}(\kappa R). \quad (2.20)$$

To completely define the solution, we choose the boundary condition  $\chi(R_c) = 0$ , resulting in discrete values for  $\kappa$ , such that  $K_{is}(\kappa_n R_c) = 0$ . For shallow bound states, where  $\kappa_n R_c \ll 1$ , the zeros of the Bessel function are given by

$$\kappa_n R_c = 2e^{-\gamma} \exp\left(-\frac{n\pi}{s}\right) [1 + \mathcal{O}(s)], \quad (2.21)$$

where  $\gamma$  is the Euler constant. Taking the ratio of consecutive  $N$ -body energies gives

$$\frac{E_N^{(n)}}{E_N^{(n+1)}} = \exp\left(\frac{2\pi}{s}\right) \quad n \rightarrow 0, 1, 2, \dots \quad (2.22)$$

Following a geometrical law just as in the three-body problem, the above equation gives us the ratios between successive  $N$ -body bound energies, even though the system under study is in a generic dimension  $D$ . In addition, we stress that the scale parameter depends on the number of light-bosons, such that, its values are distinct from that found in the three-body problem. Therefore, the log-periodic behavior of the wave function and the limit-cycles associated with correlations between observables in the  $N$ -body system built a complex pattern of interwoven cycles [36], which survives under squeezing of the system until a critical dimension by means of trap deformations. It is interesting to observe that the log-periodicity of the wave function survives for larger trap deformation when increasing the number of light-bosons, such that, in principle, one could arrive to a situation tuned by the trap deformation in which the Efimov effect is not present for three-particles, but geometrical scaling laws are still present for four or more particles. This hierarchy can be achieved close to unitarity, such that the  $N - 1$  system is in the "un-particle" regime or has continuous scale symmetry, while the  $N$ -body system has a discrete one.

The critical dimension for the Efimov effect has been already investigated by solving the Skorniakov and Ter-Martirosyan equations (STM) at the unitary limit [19]. Here, we adapt this approach by restricting it to the present situation of only heavy-light atoms resonance to allow comparison with the results from the BO approximation. In the present context, there is only one STM integral equation, which reads

$$\chi_A(q) = \tau_A \left( E_3^{(D)} - \frac{1}{2\mu_{A,AB}} q^2 \right) \times \int d^D k \frac{\chi_A(k)}{E_3^{(D)} - (k^2 + q^2)/2\mu_{AB} - \mathbf{k} \cdot \mathbf{q}/m_B}, \quad (2.23)$$

where  $\mathbf{q}$  and  $\mathbf{k}$  are defined such that their origin is the center-of-mass of a given pair and point towards the remaining particle.  $\tau_A$  is the heavy-light transition amplitude. In the limit of large momentum, the integral equation admits solutions in the form  $\chi_A(z) = C_A z^{1-D+is}$ . Substituting this homogeneous function in Eq. (2.23), one arrives to the following transcendental equation for  $s$

$$\left( \frac{2\mu_{A,AB}}{m_B} \right) \left( \frac{\mu_{AB}}{\mu_{A,AB}} \right)^{D/2} = \mathcal{F}_D I_{(D)}(s), \quad (2.24)$$

where

$$\mathcal{F}_D = \frac{1}{\Gamma(D/2 - 1)\Gamma(2 - D/2)}, \quad (2.25)$$

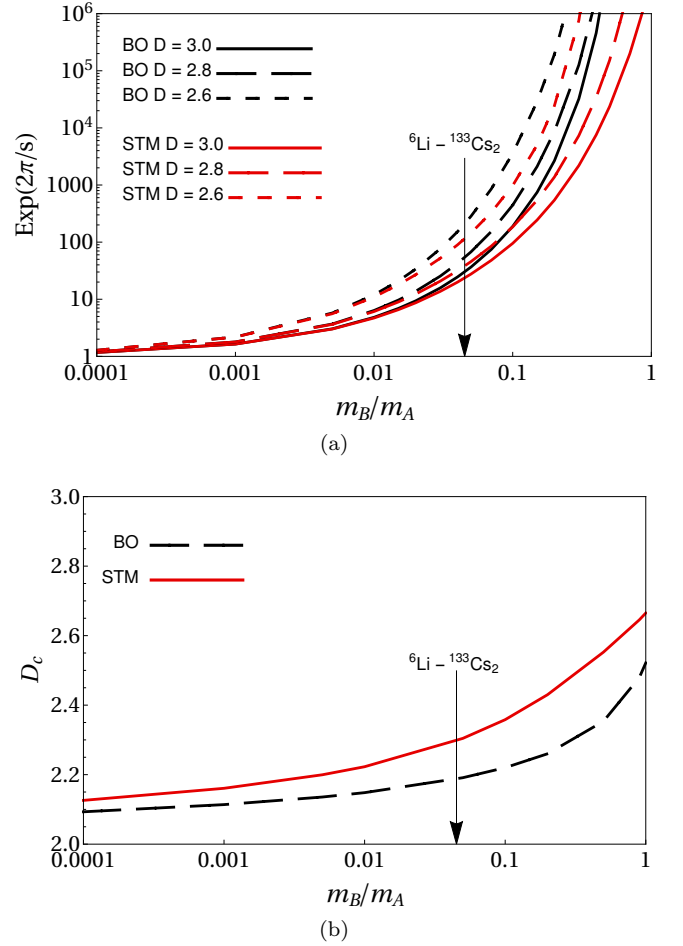


FIG. 5. Efimov effect properties for different mass ratios and dimensions for fixed null angular momentum in units of  $m_A = \hbar = 1$ . Upper panel: Efimov scale parameter in the unitary regime by means of the BO approximation compared to the solutions of Skorniakov-Ter-Martirosyan equations. Lower panel: Critical dimensions for the existence of the Efimov effect as a function of mass ratios.

and

$$I_{(D)}(s) = \int_0^\infty dz \frac{4z^{is}}{(m_B/m_A)(z^2 + 1) + (z - 1)^2} \times {}_2F_1\left(1; \frac{D-1}{2}; D-1; -\frac{4z}{(m_B/m_A)(z^2 + 1) + (z - 1)^2}\right), \quad (2.26)$$

with  ${}_2F_1(; b; c; d)$  being the ordinary (Gauss) hypergeometric function.

In Fig. 5(a), it is compared the Efimov geometric ratio between the energies of two successive states calculated by means of the BO and STM equations as a function of the mass ratio. As expected, the results of the BO approximation improves as the heavy-light mass ratio increases. Considering the three-body system to be formed by  ${}^6\text{Li}$ - ${}^{133}\text{Cs}_2$ , we find that the BO approximation overestimate the geometric ratio, while the critical dimension shown in Fig. 5(b) is underestimated on the order of 5%.



The BO approximation turns the effective interaction less attractive than it should be when comparing the results with the STM calculations, as shown in Fig. 5(a), while such behavior is reversed when approaching the critical dimension as observed in Fig. 5(b). These complex characteristics are due to the freezing of the heavy-atoms degrees of freedom in the BO approximation, while in the STM approach all the bosons are free to move.

### III. IMPURITIES BOUND STATES

Experimentally, the access to regimes where the system exhibits discrete scaling parameters is made by controlling the scattering length via Feshbach resonances, so it is interesting to write the two-body energy in terms of the respective scattering length in a generic dimension  $D$ , which ultimately would be associated to a given trap deformation. In order to accomplish this, we consider the heavy-light pair in our system to be two non-relativistic particles with a rotationally-invariant zero-range interaction. In this context, we follow closely Ref. [40]. In the zero-range model, the radial wave function for  $r > 0$  is

$$R(r) = \sqrt{\frac{\pi}{2p}} r^{\frac{2-D}{2}} \left[ \cot \delta_{(D)}(p) J_{\frac{D}{2}-1}(pr) - Y_{\frac{D}{2}-1}(pr) \right], \quad (3.1)$$

where  $r$  is the distance between the pair of particles and  $p^2/2\mu_{AB}$  is the relative energy. The phase-shift is written in terms of the scattering length by assuming that the wave function vanishes at the relative distance  $a_D$ , which gives

$$\cot \delta_D(p) = Y_{\frac{D}{2}-1}(p a_D) / J_{\frac{D}{2}-1}(p a_D). \quad (3.2)$$

For small energies, we can write

$$\cot \delta_D(p) = \cot \left( \frac{D}{2} \pi \right) - \frac{2^{D-2}}{\pi} \Gamma \left( \frac{D-2}{2} \right) \times \Gamma \left( \frac{D}{2} \right) (a_D p)^{2-D}. \quad (3.3)$$

The S-matrix in  $D$ -dimensions is written as

$$\hat{S} = \hat{1} + \left( \frac{i p}{2\pi} \right)^{\frac{D-1}{2}} \hat{f}_D(p), \quad (3.4)$$

where the scattering amplitude is given by

$$\hat{f}_D(p) = \frac{1}{p^{D-2}} \frac{1}{\cot \delta_D(p) - i}. \quad (3.5)$$

The poles of the S-matrix in the real axis are the bound states energies, and using the lowest-order effective range expansion from Eq. (3.3), one gets

$$p = i\kappa = \frac{1}{a_D} \left( \frac{2^{D-2}}{\pi} \frac{\Gamma(D/2 - 1) \Gamma(D/2)}{\cot(D\pi/2) - i} \right)^{\frac{1}{D-2}}, \quad (3.6)$$

where  $\kappa > 0$  and  $E_2^{(D)} = -\hbar^2 \kappa^2 / 2\mu_{AB}$ , which reproduces the known results [41].

So far, within the real possibilities of experimental cold-atom setups, the unitary limit is elusive, such that one has to consider finite scattering lengths in order to obtain the properties of the  $N$ -body systems close to Feshbach resonances. Taking this into account, our study is now devoted to quantify corrections out of the unitary limit and the impact of changing the effective dimension in which the system is embedded. In what follows, we will present results for few-atom bound state calculations, where the value of the scattering length  $a_D$ , or  $E_2^{(D)}$ , is the input.

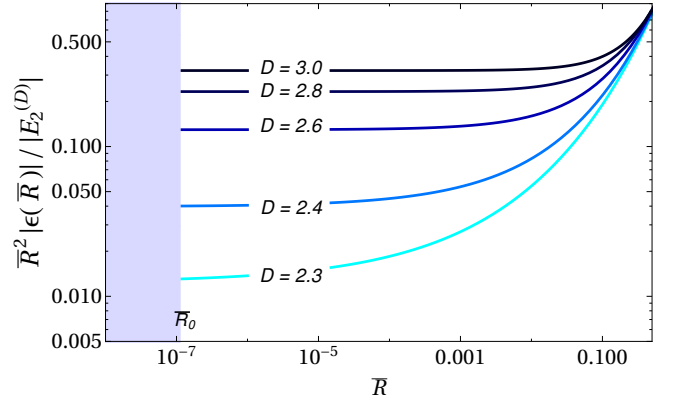


FIG. 6. Effective potential for different dimensions  $D$ . The band corresponds to the region where the short-range potential is repulsive to avoid the Thomas collapse.

In order to obtain the bound states of the two heavy-boson impurities in the cloud of  $(N-2)$ -light atoms, the heavy-heavy effective potential obtained from Eq. (2.6) has to be regularized at short distance, which is done by associating a distance  $R_0$ , named van der Waals length, with the repulsive region of real potentials. This is necessary to avoid the Thomas collapse when the condition given by Eq. (2.18) is satisfied. As an example, in cold-atomic systems,  $R_0$  is of the order of the Van der Waals radius, which determines to some extent the position of the three-atom recombination resonance, as in the case of three identical atoms [42]. Within this approach, the effective potential becomes

$$V_B(\bar{R}) = \text{sign}(\bar{R}_0 - \bar{R}) \epsilon(\bar{R}). \quad (3.7)$$

In Fig. 6, we illustrate the effective potential focusing on the  $1/R^2$  behaviour for different values of effective dimension  $D$ . As we can observe, the region where the effective potential exhibits the  $1/R^2$  behaviour diminishes as the effective dimension is decreased, so that, in principle, as the trap geometry asymmetry increases, the ratio  $R_0/a_D$  has to be tuned to lower values in order to access the geometrical scaling regime.

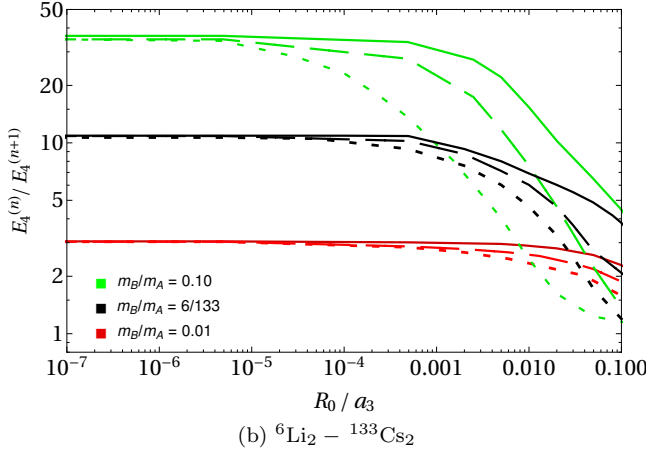
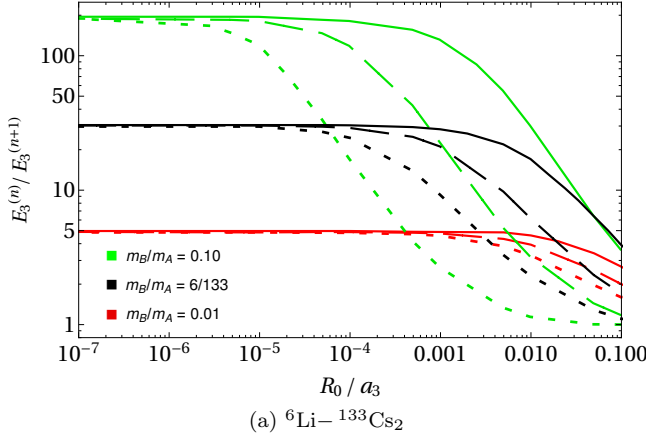


FIG. 7. Ratio between the energies of two successive states,  $E_N^{(n)}/E_N^{(n+1)}$ , as a function of  $R_0/a_3$  for dimension  $D = 3$  and angular momentum  $l = 0$ . We consider two-heavy bosonic impurities interacting with one- and two-light bosons. The solid lines corresponds to the excitation quantum number  $n = 0$ , the long-dashed  $n = 1$  and the short-dashed  $n = 2$ . The curves from top to bottom are obtained with 0.10, 6/133 and 0.01 mass ratios.

In Fig. 7, we present the ratio of two successive bound states in  $D = 3$  for (a) heavy-heavy-light and (b) heavy-heavy-light-light systems, as a function of  $R_0/a_3$  with the light-heavy mass ratios of 1/10, 6/133 and 1/100. As shown in the diagrams, for a given mass ratio and number of light atoms, when  $a_3 \gg R_0$ , the states present the geometric ratio of the form  $\exp(2\pi/s)$  and can be represented by a unique limit-cycle of the model. Besides that, we can see that the magnitude of the scattering length necessary to obtain Efimov states is smaller for the systems that present larger mass imbalances between heavy and light-atoms. This can be explained by means of the strength of the effective potential between the heavy-atoms generated by the presence of the light-

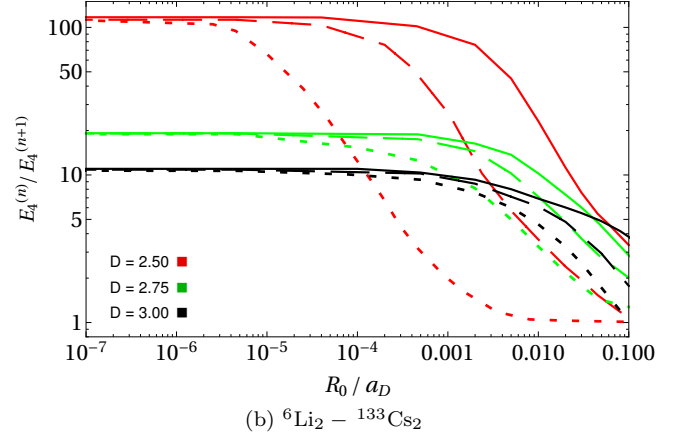
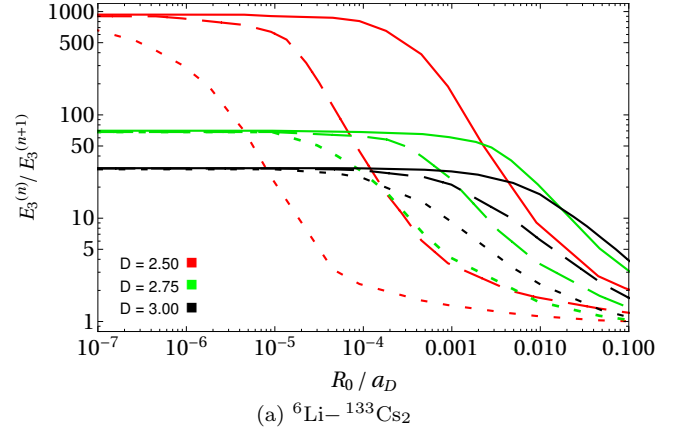


FIG. 8. Ratio between the energies of two successive states,  $E_N^{(n)}/E_N^{(n+1)}$ , as a function of  $R_0/a_D$  for fixed angular momentum  $l = 0$ . We consider two atoms of  ${}^{133}\text{Cs}$  interacting with one and two  ${}^6\text{Li}$  ones. The solid lines corresponds to the excitation quantum number  $n = 0$ , the long-dashed  $n = 1$  and the short-dashed  $n = 2$ . The curves from top to bottom are obtained for dimensions 2.5, 2.75 and 3.

ones, which is proportional to the inverse of the reduced mass  $\mu_{B,AA}$  (please see Eq. (2.8)).

Finally, as one sees by comparing figures 7(a) and 7(b), the ratio between the energy of successive states depends on the number of light-bosons. This property was also found in the four-boson system with zero-range interactions [34], and in the present model it comes from the increase of the strength of the inverse square potential in the BO approach by increasing the number of light atoms.

In Fig. 8, is shown the ratio between energies of two successive states as a function of  $R_0/a_D$ , for  ${}^6\text{Li} - {}^{133}\text{Cs}_2$  (upper panel) and  ${}^6\text{Li}_2 - {}^{133}\text{Cs}_2$  molecules (lower panel). Considering the effective dimensions 3, 2.75 and 2.5, with zero angular momentum, we have analysed up to three consecutive states, with  $n = 0, 1$  and  $2$ . As we can observe in both figures (a) and (b), as the trap is squeezed and the effective dimension decreases, the geometric ratio between successive energies increases until the criti-



cal dimension is reached. Comparing Figs. 8(a) and (b), one can observe that independently of the dimension, the discrete scale regime of the  ${}^6\text{Li}_2\text{-}^{133}\text{Cs}_2$  molecule is more resilient against the increasing of  $R_0/a_D$  when compared to the  ${}^6\text{Li-}^{133}\text{Cs}_2$  one. This can be understood since the  $1/R^2$  potential has twice the strength in the former case compared to latter one. Another aspect observed in both figures and also independent on the effective dimension, is the behaviour of the  $n+1$  energy state that changes in magnitude slowly with respect to the  $n$  one when the ratio  $R_0/a_D$  is increased. The reason for that is in the form of the effective potential, which is deep and goes with the behaviour  $1/R^2$  at short distances and is exponentially damped at large separations of the two-heavy atoms. The increase of  $R_0/a_D$  raises the kinetic energy, while pushing the state to the shallow region of the potential. The excited state, although gaining kinetic energy, does not loose considerable potential energy, while the lower state, which initially is more deep and localized in the  $1/R^2$  region, gain less kinetic energy, while looses more potential energy when it is moved to the region of the shallow potential.

In what follows, we stress the relation of the scattering length with the effective dimension, that is, aspect ratio of the trap geometry, but now, studying the wave function of the heavy-heavy pair. In Fig. 9, for different effective dimensions  $D=3$  and 2.5 (the last representing a squeezed trap with aspect ratio of  $b_{ho}/r_{2D}=1.414$ ), we illustrate the square modulus of the wave function of the pair  ${}^{133}\text{Cs-}^{133}\text{Cs}$  in the molecule  ${}^6\text{Li}_2\text{-}^{133}\text{Cs}_2$  for  $n=0, 1, 2$  and 3 energy states. The red dots represent the nodes of the highest excited state when the system is at the unitary limit. The nodes can be used as a reference on how close to the log-periodicity the system is. By comparing figures (a) and (b), the relation between the magnitude of the ratio  $R_0/a_D$  and how close the many-body energies are from the geometric scaling regime becomes evident, as squeezing the system from  $D=3$  to  $D=2.5$ , for fixed ratio  $R_0/a_D$ , makes the deviation from the logarithmic periodicity regime greater. This is in agreement with what is observed from the ratio between successive energies in Fig. 8(b).

To finalize the analysis of the many-body bound states, we show in figure 10 the scaling functions  $E_N^{(n+1)}/E_N^{(n+2)}$  vs.  $E_N^{(n)}/E_N^{(n+1)}$  for  ${}^6\text{Li-}^{133}\text{Cs}_2$  and  ${}^6\text{Li}_2\text{-}^{133}\text{Cs}_2$  molecules, exploring different effective dimensions. By changing the ratio  $R_0/a_D$ , the bound-state energies are computed from  $n=0$  up to  $n=3$ . The straight black line represents the geometric ratio in the unitary limit. The ratio of the energies for the three- and four-body reaches the continuum when becoming equal to the two-body energy and twice it, respectively. This limit is represented by the red dot in the figure. Two scaling functions for  $n=0$  and  $n=1$  are presented, the results feature the limit-cycles for three and four-particle

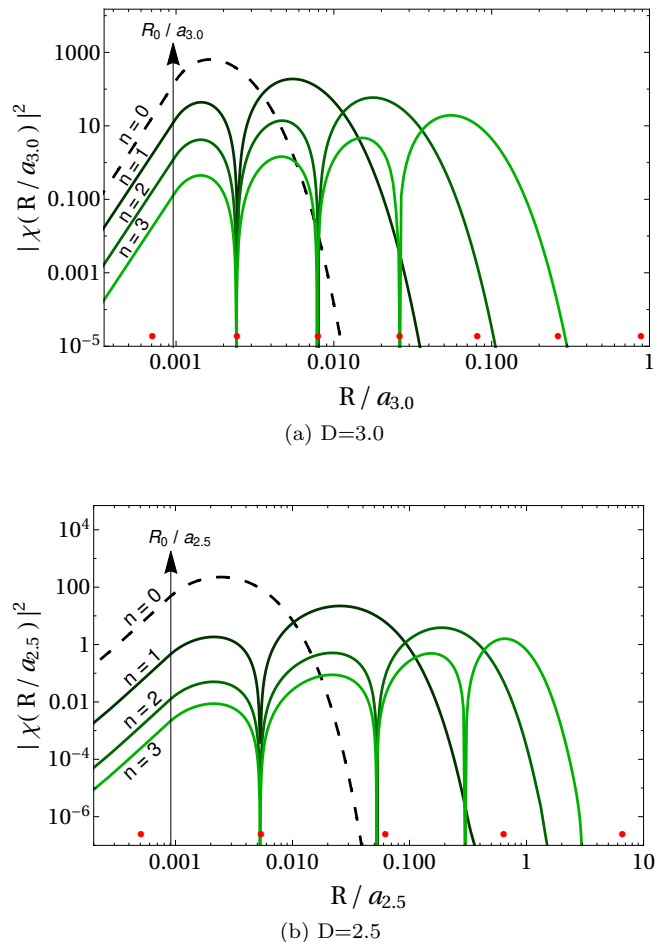


FIG. 9. Squared modulus of the bound-state wave function of the heavy-pair,  $|\chi(R/a_D)|^2$ , considering the molecule  ${}^{133}\text{Cs}_2\text{-}{}^6\text{Li}_2$  for the lowest angular momentum state. The cutoff radius in units of the scattering length is fixed in  $R_0/a_3 = 9 \times 10^{-4}$ . The ground state  $n=0$  is the dashed line, the solid lines from top to bottom are  $n=1, 2$  and 3. The red dots represent the nodes of the highest excited state when the system is at the unitary limit.

cesium-lithium systems. The limit-cycles are characteristic of the dimension and also the number of bosons. It is worthwhile to observe that the detailed form of the scaling function depends on the effective potential in the whole domain of separation between the two-heavy atoms, ranging from the short distance behavior  $1/R^2$ , to the exponential tail one.

#### IV. SUMMARY

In this work, we explored the problem of two-heavy bosonic impurities immersed in a system of light-bosons. The many-body system is embedded in  $D$  dimensions in order to mimic squeezed traps. The Hamiltonian of the system is chosen to have only zero-range heavy-

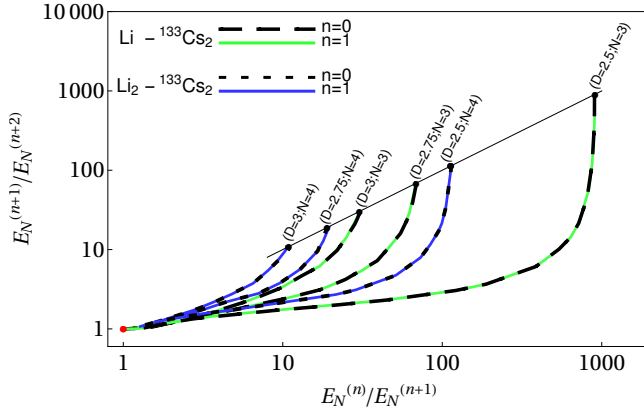


FIG. 10. Results for the scaling function  $E_N^{(n+1)}/E_N^{(n+2)}$  vs.  $E_N^{(n)}/E_N^{(n+1)}$  considering the molecules  ${}^6\text{Li}-{}^{133}\text{Cs}_2$  and  ${}^6\text{Li}_2-{}^{133}\text{Cs}_2$  for  $n = 0$  and  $n = 1$ . The three- and four-body system is squeezed in different effective dimensions. The straight line is the unitary limit. The red dot is the limit where the states reaches the continuum.

light interactions, which can be treated within the Born-Oppenheimer approach to compute the bound state energy and wave function. Correlations between the many-body bound state energies for different dimension, mass ratio and number of light-bosons are discussed. The study have focused in the limit of discrete scale symmetry to a continuous one considering both zero and finite heavy-light bound energies.

We have found that the effective dimension point associated to a squeezed trap limit where the discrete scale symmetry breaks to the continuum one, depends on several system variables, such as, the angular momentum, the number of light-bosons and the mass imbalance between heavy-light pairs. As an example, we can find situations in squeezed traps where systems with three bosons are out of the discrete scaling symmetry regime, while four or more bosons are still in. Besides that, the angular momentum of the heavy system, which tends to destroy the discrete scale symmetry regime can be balanced by the number of light-bosons. Furthermore, if the two-heavy bosonic impurities are substituted by two-fermionic ones in only one spin state, discrete scale symmetries can still be present if the number of light-bosons is large enough, on the side of the mass imbalance.

Noteworthy is the control of the trap aspect ratio that would allow, in principle, a situation where the interwoven cycles of systems with different number of light-bosons can be disentangled, by engineering the trap in a particular way. On the top of that, it would still be possible to have tunable induced many-body forces [43] close to narrow Feshbach resonances, which would add another control to manipulate the few-body scales in an independent way within cold few-atom systems, besides the aspect ratio, the number of particles and angular momentum. Furthermore, below the critical dimension or

large angular momentum of the pair, the continuum scale symmetry in the unitary limit is valid, which is associated with the "unparticle physics" regime [44] already explored in the context of nuclear physics [39]. It could be that if we take a light-particle out of the system at unitarity limit, while the original one has still discrete scale symmetry, the one with less atoms has a continuum one. These are interesting findings to take into account when planning or developing future experiments with the aim of observe the discrete and continuum scaling in processes involving three and more atoms in squeezed cold atomic traps.

We have placed our study in the context of the  ${}^6\text{Li}_{N-2}{}^{133}\text{Cs}_2$  molecule, where the  ${}^6\text{Li}-{}^6\text{Li}$  interaction is weak, which would be the case when the scattering length vanishes. In the particular case of  $N = 3$  by means of the Born-Oppenheimer approximation in different dimensions, we computed for the lowest angular momentum state at the unitarity limit the critical dimension where the Efimov effect vanishes ( $D_c \simeq 2.188$ ), which represents an overestimation of 5% over the Skorniakov and Ter-Martirosian result ( $D_c \simeq 2.298$ ). For  $N = 3$  and  $N = 4$ , we also study the  ${}^{133}\text{Cs}-{}^{133}\text{Cs}$  wave function up to three excited states for some effective dimensions and different ratios between the short-range cutoff ( $R_0$ ) and the heavy-light scattering length ( $a_D$ ). We found that the tune of  $R_0/a_D$ , necessary to place the system into the discrete scale regime, is strongly correlated to the aspect geometry of the trap, that is associated to the effective dimension in which the system is embedded. Finally, we checked the formation of the limit cycles in the correlation of  $E_N^{(n+1)}/E_N^{(n+2)}$  vs.  $E_N^{(n)}/E_N^{(n+1)}$ . These correlations and the corresponding limit-cycles are limited to the existence of the bound system  ${}^6\text{Li}-{}^{133}\text{Cs}$  and at the present stage we have not introduced the three-body threshold properly in the calculations for the  ${}^6\text{Li}_2{}^{133}\text{Cs}_2$  system.

In summary, our study corroborates with the existence of geometrical scaling laws for  $N$ -body systems with different log-periodicity properties for each system configuration. Such properties were also found in Ref. [34] for four identical-atoms with non-zero interactions in momentum space. Hence, for future works, we plan to introduce a non-zero interaction between the light-particles into our system in coordinate space, which makes the problem much more difficult to solve in mathematical terms and could bring some corrections to the quantities that we have found in the present paper.

## ACKNOWLEDGMENTS

This work was partially supported by Fundação de Amparo à Pesquisa do Estado de São Paulo (FAPESP) [Grants No. 2017/05660-0 (T.F.) and No. 2020/00560-0 (D.S.R.)], Conselho Nacional de Desenvolvimento Científico e Tecnológico (CNPq) [Grants No. 308486/2015-3 (T.F.)], and Fundação de Amparo à Pesquisa do Estado de Minas Gerais (FAPEMIG) [Grants No. 11608].

- 
- [1] V. Efimov, Phys. Lett. B **33**, 563 (1970).
  - [2] T. Kraemer, M. Mark, P. Waldburger, J. G. Danzl, C. Chin, B. Engeser, A. D. Lange, K. Pilch, A. Jaakkola, H.-C. Ngerl and R. Grimm, Nature **440**, 315 (2006).
  - [3] B. Huang, L. A. Sidorenkov, R. Grimm and J. M. Hutson, Phys. Rev. Lett. **112**, 190401 (2014).
  - [4] J. R. Williams, E. L. Hazlett, J. H. Huckans, R. W. Stites, Y. Zhang, and K. M. O'Hara, Phys. Rev. Lett. **103**, 130404 (2009).
  - [5] T. Kraemer, M. Mark, P. Waldburger, J. G. Danzl, C. Chin, B. Engeser, A. D. Lange, K. Pilch, A. Jaakkola, H.-C. Nägerl, and R. Grimm, Nature **440**, 315 (2006).
  - [6] R. Pires, J. Ulmanis, S. Häfner, M. Repp, A. Arias, E. D. Kuhnle, and M. Weidemüller, Phys. Rev. Lett. **112**, 250404 (2014).
  - [7] S.-K. Tung, K. Jiménez-García, J. Johansen, C. V. Parker and C. Chin, Phys. Rev. Lett. **113**, 240402 (2014).
  - [8] Ruth S. Bloom, Ming-Guang Hu, Tyler D. Cumby and D. S. Jin, Phys. Rev. Lett. **111**, 105301 (2013).
  - [9] E. Braaten, and H. W. Hammer, Annals Phys. **322**, 120 (2007).
  - [10] M. Sun, H. Zhai and X. Cui, Phys. Rev. Lett. **119**, 013401 (2017).
  - [11] S. Moroz, J. P. D'Incao and Dmitry S. Petrov, Phys. Rev. Lett. **115**, 180406 (2015).
  - [12] M. J. Gullans, S. Diehl, S. T. Ittenhouse, B. P. Ruzic, J. P. D'Incao, P. Julienne, A. V. Gorshkov and J. M. Taylor, Phys. Rev. Lett. **119**, 233601 (2017).
  - [13] E. Nielsen, D. V. Fedorov, A. S. Jensen and E. Garrido, Phys. Rep. **347**, 373 (2001).
  - [14] E. Braaten and H. W. Hammer, Phys. Rept. **428**, 259 (2006).
  - [15] T. Frederico, A. Delfino, L. Tomio and M. T. Yamashita, Prog. Part. Nucl. Phys. **67**, 939 (2012).
  - [16] P. Naidon and S. Endo, Rept. Prog. Phys. **80**, 056001 (2017).
  - [17] C. H. Greene, P. Giannakeas and J. Perez-Rios, Rev. Mod. Phys. **89**, 035006 (2017).
  - [18] L. H. Thomas, Phys. Rev. **47**, 903 (1935).
  - [19] D. S. Rosa, T. Frederico, G. Krein, and M. T. Yamashita, Phys. Rev. A **97**, 050701(R) (2018). *Erratum*, Phys. Rev. A **104**, 029901 (2021).
  - [20] A. Mohapatra and E. Braaten, Phys. Rev. A **98**, 013633 (2018).
  - [21] E. R. Christensen, A. S. Jensen, E. Garrido, Few-Body Syst. **59**, 136 (2018).
  - [22] D. S. Rosa, T. Frederico, G. Krein, M. T. Yamashita, J. Phys. B At. Mol. Opt. Phys. **52**, 025101 (2018).
  - [23] J. H. Sandoval, F. F. Bellotti, M. T. Yamashita, T. Frederico, D. V. Fedorov, A. S. Jensen and N. T. Zinner, J. Phys. B: At. Mol. Opt. Phys. **51**, 065004 (2018).
  - [24] E. Garrido and A.S. Jensen, Phys. Rev. Res. **2**, 033261 (2020).
  - [25] D. S. Petrov, M. Holzmann and G. V. Shlyapnikov, Phys. Rev. Lett. **84**, 2551 (2000).
  - [26] M. Greiner, I. Bloch, O. Mandel, T. W. Hänsch and T. Esslinger, Appl. Phys. B **73**, 769 (2001).
  - [27] H. Kröger and R. Perne, Phys. Rev. C **22**, 21 (1980).
  - [28] S. K. Adhikari and A. C. Fonseca, Phys. Rev. D **24**, 416 (1981).
  - [29] H. W. L. Naus and J. A. Tjon, Few-Body Syst. **2**, 121 (1987).
  - [30] M. T. Yamashita, D. V. Fedorov and A. S. Jensen, Phys. Rev. A **81**, 063607 (2010).
  - [31] M. T. Yamashita, L. Tomio, A. Delfino and T. Frederico, Europhys. Lett. **75**, 555 (2006).
  - [32] J. von Stecher, Phys. Rev. Lett. **107**, 200402 (2011).
  - [33] Y. Yan and D. Blume, Phys. Rev. A **92**, 033626 (2015).
  - [34] M. R. Hadizadeh, M. T. Yamashita, L. Tomio, A. Delfino, and T. Frederico, Phys. Rev. Lett. **107**, 135304 (2011).
  - [35] M. R. Hadizadeh, M. T. Yamashita, L. Tomio, A. Delfino, and T. Frederico, Phys. Rev. A **87**, 013620 (2013).
  - [36] W. De Paula, A. Delfino, T. Frederico and L. Tomio, J. Phys. B **53**, 205301 (2020).
  - [37] P. Naidon, Few-Body Syst **59**, 64 (2018).
  - [38] L. D. Landau, and E. M. Lifshitz, *Quantum Mechanics* (Pergamon Press, London, 1977).
  - [39] H. W. Hammer and D. T. Son, Proc. Nat. Acad. Sci. **118**, e2108716118 (2021). [arXiv:2103.12610 [nucl-th]].
  - [40] H.-W. Hammer and D. Lee, Phys. Lett. B **681**, 500 (2009).
  - [41] M. Valiente, N. T. Zinner and K. Mølmer, Phys. Rev. A **86**, 043616 (2012).
  - [42] J. Johansen, B. J. Desalvo, K. Patel, and C. Chin, Nature Physics **13**, 731 (2017).
  - [43] M. T. Yamashita, T. Frederico, and L. Tomio, Braz. J. Phys. **51**, 277 (2021).
  - [44] H. Georgi, Phys. Rev. Lett. **98**, 221601 (2007).